ISSN 0036-0236, Russian Journal of Inorganic Chemistry, 2007, Vol. 52, No. 5, pp. 761–767. © Pleiades Publishing, Inc., 2007.
Original Russian Text © D.M. Babanly, Yu.A. Yusibov, M.B. Babanly, 2007, published in Zhurnal Neorganicheskoi Khimii, 2007, Vol. 52, No. 5, pp. 827–833.

PHYSICOCHEMICAL ANALYSIS OF INORGANIC SYSTEMS

Phase Equilibria and Thermodynamic Properties of the System Tl–TlBr–Se

D. M. Babanly, Yu. A. Yusibov, and M. B. Babanly

Rasul-zade State University, Khalilov av. 23, Baku, 370148 Azerbaijan

Received January 28, 2006

Abstract—The system Tl–Se–Br was studied in the region Tl–TlBr–Se by DTA, X-ray powder diffraction, emf measurements, and microhardness measurements. Several vertical sections, the isothermal section at 400 K, and the liquidus-surface projection were constructed. The quasi-binary sections TlBr–Tl_2Se, TlBr–TlSe, Tl_5Se_2Br–Tl, and Tl_5Se_2Br–TlSe allow the system Tl–TlBr–Se to be triangulated into five subordinate triangles. Wide immiscibility regions were discovered in the system, including a three-phase region in subsystem Tl_2Br–Tl_2Se–Se. Homogeneity and primary separation regions were determined, as well as the types and coordinates of invariant and monovariant equilibria on the *T–x–y-* diagram. From the results of emf measurements, the standard thermodynamic functions of formation were calculated for the compound Tl_5Se_2Br.

DOI: 10.1134/S0036023607050178

Here, we continue our physicochemical investigation of thallium chalcogenides started in [1–8] and present new data on the phase equilibria and thermodynamic properties of the system Tl–Se-Br in the region Tl–TlBr–Se.

The system Tl–Se–Br was studied in several works. In work [9], the quasi-binary section TlBr–Tl_2Se was described, in which the congruently melting compound Tl_5Se_2Br is formed (745 K) with a virtually constant composition. This compound forms a eutectic (~10 mol % Tl_2Se, 705 K) with TlBr and a peritectic (90 mol % Tl_2Se, 720 K) with Tl_2Se. The peritectic reaction $L + Tl_5Se_2Br \rightleftharpoons \alpha$ produces the Tl_2Se-base α phase, whose homogeneity region at 720 K reaches ~25 mol % TlBr.

According to the data in work [10], the system TlBr–TlSe is also quasi-binary and has a simple eutectic phase diagram. The eutectic has the composition 90 mol % TlSe and temperature 595 K. The restudy of this system [7] showed eutectic equilibrium (85 mol % TlSe, 580 K) and monotectic equilibria. At the monotectic temperature (690 K), the immiscibility region extends from 20 to 50 mol % TlSe[7]. The vertical sections $0.25Tl_5Se_2Br$–TlSe and Tl_5Se_2Br–Tl are also quasi-binary [8]. The former is of the eutectic type (60 mol % TlSe, 590 K) with an extensive region (to 13 mol % TlSe) of Tl_5Se_2Br-base solid solution; the latter has a monotectic phase diagram (733 K) with a degenerate eutectic.

In work [11], the crystal structure of Tl_5Se_2Br was studied. This compound has a tetragonal Tl_5Te_3-type structure (space group *I*4/*mcm*) [12] with the following unit cell parameters: a = 8.594 Å, c = 12.788 Å, Z = 4.

EXPERIMENTAL

First, the compounds TlBr, Tl_2Se, TlSe, and Tl_5Se_2Br were prepared. Tl_2Se and TlSe were synthesized by the ampoule technique from the high-purity constituent elements (10^{-3} wt % impurities) under vacuum (~10^{-2} Pa). The alloying temperature was 750 K.

Thallium monobromide was prepared as described in work [13]. First, metallic thallium was dissolved at ~350 K in dilute (~7–10 M) sulfuric acid to obtain a Tl_2SO_4 solution. Then, to the boiling 2% Tl_2SO_4 solution, dilute HBr was added until reaching complete precipitation. TlBr is hardly recrystallizable. Therefore, the trace mother solution was removed by repeated boiling with water; then, it was filtered and sucked. The product was dried over KOH in a desiccator at 390–400 and stored in the dark to avoid its degradation.

Alloying the thus prepared TlBr with elementary thallium and selenium in required proportions in a evacuated silica ampoule, we obtained the ternary compound Tl_5Se_2Br.

All compounds synthesized were identified by DTA and X-ray powder diffraction.

Alloying the precursor compounds with elementary selenium and thallium in various proportions in evacuated silica ampoules, we prepared alloys with compositions lying along the sections TlBr–Tl_2Se, TlBr–Se, Tl_2Se–[Tl_2Br] (hereafter, heterogeneous alloys taken as a "component" are indicated in parentheses), Tl_2Se–[TlSeBr], and Tl_5Se_2Br–Se, as well as several samples in the region Tl–TlBr–Se. The compositions of these samples were chosen proceeding from the available phase equilibrium data in the boundary binary Tl–Se [14, 15] and along the previously studied inner

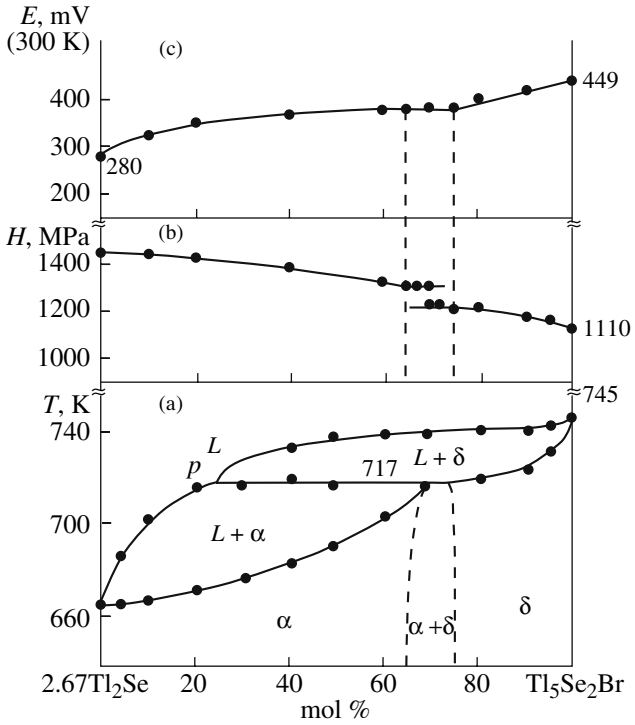

Fig. 1. (a) T–x, (b) H_μ–x, and (c) E–x diagrams for the system Tl_2Se–Tl_2Se_2Br.

sections of the ternary system [7–9]. For equilibration, the alloys were annealed at temperatures 20–30 K below the solidus for 500–1000 h.

The investigation of selected samples along the section TlBr–Tl_2Se showed that in the region TlBr–Tl_5Se_2Br, data coincided with the data of work [9] but were slightly different in the subsystem Tl_5Se_2Br–Tl_2Se. In view of this, we restudied the system Tl_5Se_2Br–Tl_2Se. Particular attention was paid to the equilibration of alloys. After being alloyed at 780–800 K, samples were homogenized by stepwise annealing: first, they were annealed at 690 K for 500 h, then cooled to 650 K and exposed at this temperature for 500 h. Transitions between the specified temperatures were very slow (for ~10 h).

The investigative tools used were DTA (pyrometer NTR–75, chromel–alumel thermocouples), X-ray powder diffraction (diffractometer DRON-2, CuK_α radiation), microhardness measurements (tester PM~T-3), and emf measurements in the concentration circuits

$$\begin{array}{l}(-)\ \text{Tl solid/liquid electrolyte}\\ +\ \text{Tl}^+/(\text{Tl–Se–Br})\ (\text{solid})(+)\end{array} \qquad (1)$$

from 300 to 430 K. The electrolyte was a glycerol solution of KBr with ~0.5 wt % TlBr. The left-hand electrode was metallic thallium. The right-hand electrodes were presynthesized equilibrium alloys from the region TlBr–Tl_2Se–Se of the system Tl–TlBr–Se.

The emf was measured by a compensation technique using a high-resistance digital voltmeter V-7-34A. The composition of circuits (1) and the emf measurement procedure were the same as in works [5, 15].

RESULTS AND DISCUSSION

Figure 1 displays the results of the investigation of Tl_5Se_2Br–Tl_2Se alloys after careful heat treatment. Our design of the phase diagram (Fig. 1a) differs from that in work [9] in that the Tl_5Se_2Br-base δ phase of variable composition exists along with the Tl_2Se-base α solid solution. There is peritectic equilibrium $Lp + \delta \rightleftharpoons \alpha$ (T = 717 K). The peritectic point p has the composition ~25 mol % Tl_5Se_2Br. The coordinates of all invariant equilibria of the system Tl–TlBr–Se are compiled in Table 1 and are not specified in the text.

The microhadrness (Fig. 1b) and emf measurements (Fig. 1c) and X-ray powder diffraction data verify the single-phase composition of alloys in the region 0–65 mol % Tl_5Se_2Br (α phase) and 75–100 mol % Tl_5Se_2Br (δ phase).

In the homogeneity region of the α phase, the microhardness decreases from ~1450 MPa in pure Tl_2Se to ~1300 MPa; in the region of the δ phase, it increases from 1100 MPa in Tl_5Se_2Br to 1200 MPa (Fig. 1b). The emf isotherm at 300 K consists of two monotonic curves in the ranges 0–65 and 75–100 mol % Tl_5Se_2Br. In the range 65–75 mol % Tl_5Se_2Br, the emf has a fixed value ((390 ± 2) mV), indicating the constancy of the compositions of the α- and δ phases, i.e., the two-phase (α + δ) constitution of the alloys [15].

The indexing of X-ray powder diffraction patterns shows that the in the homogeneity region of the α phase (0–65 mol % Tl_5Se_2Br), the alloys have a tetragonal Tl_5Se_{3-x}-type structure (space group $P4/ncc$) [16] and that their unit cell parameters vary monotonically in the following ranges: a = 8.523–8.555 Å, c = 12.68–12.73 Å. Within the homogeneity region of the δ phase (75–100 mol % Tl_5Se_2Br), the unit cell parameters of the Tl_5Te_3-type tetragonal lattice [12] have the following values: a = 8.571–8.595 Å, c = 12.75–12.79 Å.

The section 0.5TlBr–Se (Fig. 2) is quasi-binary and monotectic type (m_4.) At the monotectic temperature (723 K), the immiscibility region extends from 6 to ~99 at. % Se. The eutectic (494 K) is degenerate near pure selenium.

The vertical sections [Tl_2Br]–Tl_2Se (Fig. 3), 0.125Tl_5Se_2Br–Se (Fig. 4), and Tl_2Se–[TlSeBr] (Fig. 5) have complicated interactions and reflect almost all invariant and monovariant equilibria of the system Tl–TlBr–Se.

The section [Tl_2Br]–Tl_2Se crosses the subsystems Tl–TlBr–Tl_5Se_2Br and Tl–Tl_5Se_2Br–Tl_2Se. Its characteristic feature is an extensive (0–85 mol % Tl_2Se) two-phase liquid immiscibility region ($L_1 + L_2$). The hori-

zontals at 700 and 710 K are due to four-phase monotectic equilibria (Table 1, Fig. 6; $M_1M_1^*$ and $M_2M_2^*$. The DTA curves for almost all alloys show well-defined peaks at 575 and 505 K associated with the crystallization and polymorphic transition of elementary thallium (Fig. 3); the appearance of these peaks signifies the degeneracy of the suggested eutectics of the subsystems Tl–TlBr–Tl_5Se_2Br and Tl–Tl_5Se_2Br–Tl_2Se near the thallium corner of the triangle.

The section **0.125Tl_5Se_2Br–Se** (Fig. 4) crosses the subordinate triangles TlBr–Tl_5Se_2Br–TlSe and TlBr–TlSe–Se and reflects several invariant equilibria (E, e_5, e_2, m_2) and monovariant equilibria (Fig. 6; Tables 1, 2). The liquidus consists of three branches associated with the primary crystallization of TlBr and the Tl_5Se_2Br-base δ phase and selenium. The liquidus of the δ phase covers the range 0–2.0 at. % Se. In the range ~60–98 mol % Se, TlBr crystallizes by the monovariant monotectic reaction $L_2 \rightleftarrows L_3$ + TlBr (Table 2, Fig. 6; curve $M'_T m_2$).

The section Tl_2Se–[TlSeBr] (Fig. 5) is more complex. The section crosses three subordinate triangles and reflects eutectic (e_4, e_5, E) and monotectic M_T, m_2) invariant equilibria, as well as several monovariant equilibria (Fig. 6; Tables 1, 2). Along this section, Tl_2Se has an extensive α homogeneity range (85–100 mol % Tl_2Se). The liquidus consists of the primary crystallization areas of the compound TlBr (0–65 mol % Tl_2Se), α phase, and δ phase. We failed to clearly demarcate the last two fields. In Fig. 5, the phase fields with the participation of these phases are demarcated by dashed lines with account for the subsolidus fields α + TlSe and δ + TlSe (Fig. 7). This section reflects immiscibility regions, including the three-phase region $L_2 + L'_2 + L_3$ (for more detail, see the description of the liquidus-surface projection below).

The subsolidus phase fields of the system Tl–TlBr–Se are displayed in Fig. 7. The α- and δ phases have extensive homogeneity regions. These regions are separated by a narrow two-phase region α + δ, which narrows with increasing selenium concentration and practically degenerates to transform into the morphotropic phase transition α ⇄ δ. In Fig. 7, there are four two-phase fields: Tl_1 + α, Tl_1 + δ, α + TlSe and δ + TlSe. The first two fields are separated by a narrow three-phase field Tl_1 + α + δ; a possible three-phase field α + δ + TlSe is degenerate (shown in dashed lines).

The liquidus surface of the system Tl–TlBr–Se (Fig. 6) consists of three major fields associated with the primary crystallization of TlBr, the δ phase, and TlSe (fields *1–3*). The α phase field is a narrow band extending along the Tl–Se binary (field *4*). The liquidus surfaces of elementary thallium and selenium are degenerate at the relevant corners of the triangular diagram (Fig. 6).

Table 1. Invariant equilibria of the system Tl–TlBr–Se

Point in Fig. 6	Equilibrium	Composition, at. %		T, K
		Br	Se	
D_1	L ⇄ Tl_2Se	–	33.3	663
D_2	L ⇄ TlSe	–	50	617
D_3	L ⇄ TlBr	50	–	733
D_4	L ⇄ Tl_5Se_2Br (δ)	12.5	25	745
e_1	L ⇄ Tl_2Se(α) + TlSe	–	43	580
e_2	L ⇄ TlSe + Se	–	73	475
e_3	L ⇄ TlBr + δ	43	4.5	705
e_4	L ⇄ δ + TlSe	5	40.5	590
e_5	L ⇄ TlBr + TlSe	7.5	42.5	580
E	L ⇄ δ + TlBr + TlSe	7.5	41	573
p	L + δ ⇄ α	3	31	717
$m_1(m_1^*)$	L_2 ⇄ L_1 + Tl_2Se(α)	–	32.5	653
$m_2(m'_2)$	L_3 ⇄ L'_2 + Se	–	97.5(77)	487
$m_3(m_3^*)$	L_2 ⇄ L_1 + TlBr	49	–	730
$m_4(m_4^*)$	L_2 ⇄ L_3 + TlBr	47	6	723
$m_5(m_5^*)$	L_2 ⇄ L_1 + Tl_5Se_2Br(δ)	11.5	23	728
$m_6(m'_6)$	L_2 ⇄ ж'$_2$ + TlBr	40(25)	10(25)	690
$M_1(M_1^*)$	L_2 ⇄ L_1 + TlBr + δ	42	4	700
$M_2(M_2^*)$	L_2 + δ ⇄ L_1 + α	2.5	30	710
$M_3(M'_3)$	L_2 ⇄ L'_2 + TlBr + δ	38(27)	10(21)	675
$M_T(M'_T, M_T^*)$	L_2 ⇄ L'_2 + L_3 + TlBr	41.5(7)	10(66)	680

Notes: Conjugate invariant points and their compositions are parenthesized. Asterisks mark points degenerate at elementary thallium or selenium. α and δ denote solid solutions based on Tl_2Se and Ti_2Se_2Br, respectively.

According to the Kurnakov's principle of congruent triangulation [17], the T–x–y diagram of the system Tl–TlBr–Se can be considered as the combination of the following autonomous subsystems: Tl–TlBr–Tl_5Se_2Br (I), Tl–Tl_2Se–Tl_5Se_2Br (II), TlBr–Tl_5Se_2Br–TlSe (III), Tl_2Se–TlSe–Tl_5Se_2Br (IV), and TlBr–TlSe–Se (V).

The liquidus surfaces of the subsystems **I** and **II** are almost fully covered by the immiscibility region $L_1 + L_2$. The intersection of this region by the eutectic curve (e_3M_2)

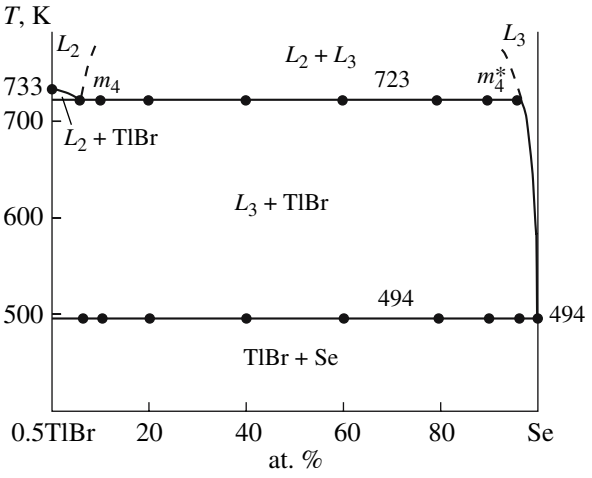

Fig. 2. TlBr–Se phase diagram.

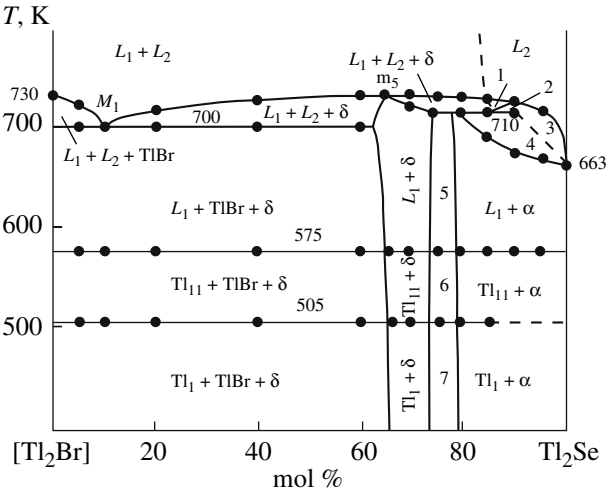

Fig. 3. Vertical section $[Tl_2Br]$–Tl_2Se of the Tl–TlBr–Se phase diagram. Phase fields: (*1*) $L + \delta$, (*2*) $L + \alpha + \delta$, (*3*) $L + \alpha$, (*4*) $L_1 + L_2 + \alpha$, (*5*) $L_1 + \alpha + \delta$, (*6*) $Tl_{11} + \alpha + \delta$, and (*7*) $Tl_1 + \alpha + \delta$.

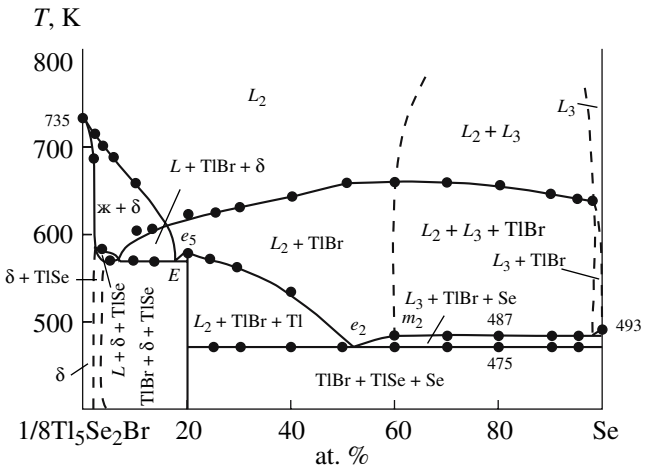

Fig. 4. Vertical section Tl_5Se_2Br–Se of the Tl–TlBr–Se phase diagram.

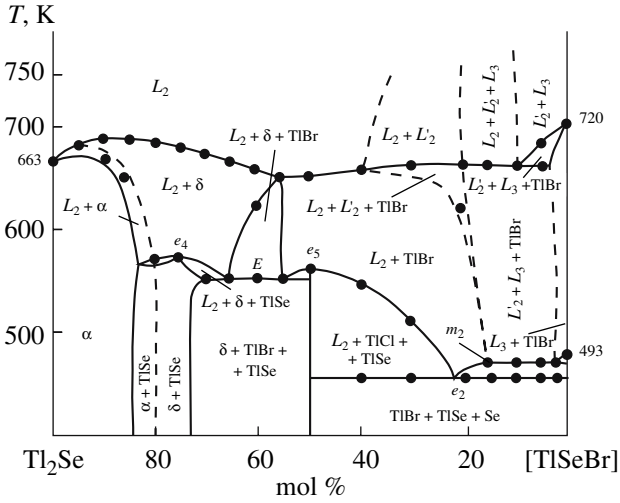

Fig. 5. Vertical section Tl_2Se–[TlSeBr] of the Tl–TlBr–Se phase diagram.

and the peritectic curve (pM_2) leads to four-phase monotectic equilibria M_1 and M_2, respectively (Tables 1, 2). Conjugate points M_1^* and M_2^* (Table 1), which correspond to the compositions of the liquid phase L_1, are virtually degenerate at the thallium corner of the triangle. Eutectic equilibrium ($L_1 \rightleftharpoons Tl_1 + TlBr + \delta$) and peritectic equilibrium ($L_1 + \delta \rightleftharpoons Tl_1 + \alpha$), which correspond to the full solidification of melts, are also degenerate.

The subsystem **III** also has liquid–liquid immiscibility ($m_6M_3KM_3'm_6'$), which is due to the penetration of the immiscibility region m_6m_6' along the quasibinary section TlBr–TlSe into this subsystem. The eutectic curve e_3E splits into a pair of curves (e_3M_3 and $M_3'E$) when intersecting this region to form the horizontal M_3M_3' with monotectic invariant equilibrium. Solidification ends with eutectic equilibrium E (Table 1).

The subsystem **IV** involves eutectic invariant equilibrium e_4e_1. A possible peritectic reaction $L + \delta \rightleftharpoons \alpha$ has not been detected experimentally, apparently because of the degeneracy of the two-phase field $\alpha + \delta$ in this subsystem (Fig. 7).

The subsystem *V* (Fig. 6) has an extensive three-phase immiscibility region $L_1 + L_2' + L_3$ (triangle $M_TM_T'M_T^*$), in which TlBr crystallization occurs by the monotectic invariant reaction (Table 1). This trian-

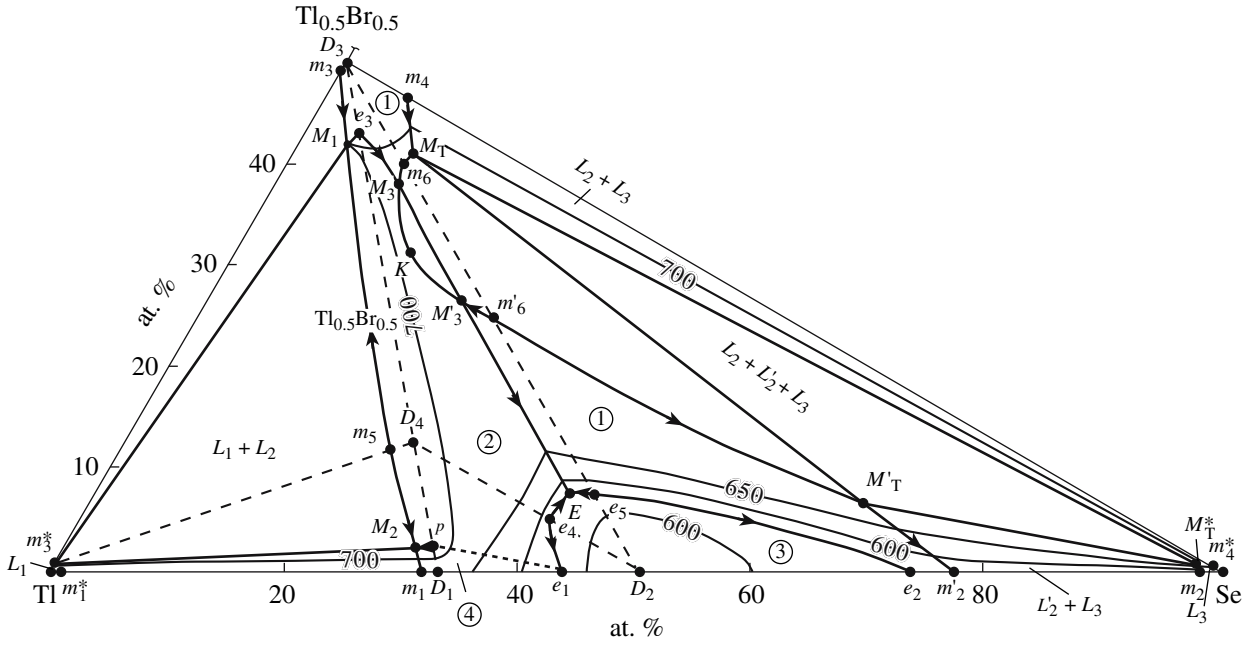

Fig. 6. Liquidus surface projection for the system Tl–TlBr–Se. Primary crystallization fields: (*1*) TlBr, (*2*) Tl_5Se_2Br-base δ phase, (*3*) TlSe, and (*4*) Tl_2Se-base α phase. Quasi-binary joins are indicated by dashed lines.

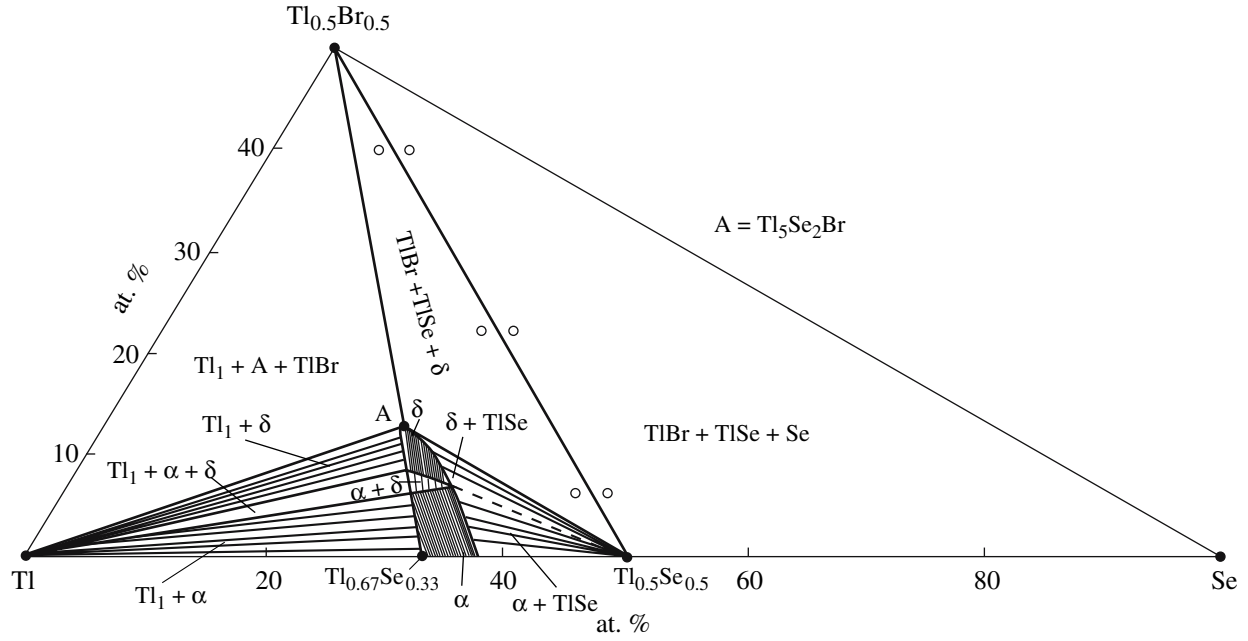

Fig. 7. Isothermal section at 400 K of the Tl–TlBr–Se phase diagram. Dashed lines indicate the boundary between the two-phase fields α + TlSe and δ + TlSe. Circles indicate the compositions of the alloys studied by the emf method.

gle by its three sides bounds the immiscibility regions $L_2 + L'_2$ ($m_6M_TM'_Tm'_6$), $L_2 + L_3$ ($m_4M_TM^*_Tm^*_4$), and $L'_2 + L_3$ ($M'_Tm_2m^*_2M^*_T$) that originate from the boundary binaries of the subsystem **V**. Four-phase eutectic equilibrium $L \rightleftharpoons$ TlBr+ TlSe + Se is degenerate near point e_2.

Along with verifying the subsolidus equilibrium phase diagram for the system TlBr–Tl_2Se–Se, the emf technique determined the thermodynamic functions for the compound Tl_5Se_2Br. In view of the linear trend of the emf versus temperature, the results of the emf measurements for circuit (1) in the region TlBr Tl_5–Se_2Br–

Table 2. Monovariant equilibria of the system Tl–TlBr–Se

Curve in Fig. 6	Equilibrium	Temperature range, K
e_3M_1	$L \rightleftarrows TlBr + \delta$	705–700
e_3M_3	$L \rightleftarrows TlBr + \delta$	705–675
e_4e_1	$L \rightleftarrows \delta + TlSe$	590–580
e_4E	$L \rightleftarrows (\delta)\alpha + TlSe$	590–573
e_5E	$L \rightleftarrows TlBr + TlSe$	580–573
e_5e_2	$L \rightleftarrows TlBr + TlSe$	580–475
PM_2	$L + \delta \rightleftarrows \alpha$	717–710
M_2m_1	$L_2 \rightleftarrows L_1 + \alpha$	713–653
m_3M_1	$L_2 \rightleftarrows L_1 + TlBr$	730–700
m_4M_T	$L_2 \rightleftarrows L_3 + TlBr$	723–680
m_5M_1	$L_2 \rightleftarrows L_1 + Tl_5Se_2Br(\delta)$	728–700
m_5M_2	$L_2 \rightleftarrows L_1 + \delta$	728–710
$m_6M_3(m_6' M_3')$	$L_2 \rightleftarrows L_2' + TlBr$	690–675
$m_6M_T(m_6' M_T')$	$L_2 \rightleftarrows L_2' + TlBr$	690–680
$M_T'm_2$	$L_2' \rightleftarrows L_3 + TlBr$	680–487

Note: Conjugate monotectic curves are in parentheses.

TlSe were processed by least-squares fits [15, 18] and presented, in accordance with recommendation in [19], in the form of

$$E = 464.7 - 0.053T$$
$$\pm 2[(0.93/22) + 3\times10^{-5}(T - 362.8)^2]^{1/2}.$$

Using known thermodynamic relationships, from this equation we calculated the relative partial molar functions for thallium in the region TlBr–Tl_5Se_2Br–TlSe at 298 K:

$$\Delta\bar{G}_{Tl} = -(43.32 \pm 0.06) \quad \text{kJ/mol},$$

$$\Delta\bar{H}_{Tl} = -(44.84 \pm 0.39) \quad \text{kJ/mol},$$

$$\Delta\bar{S}_{Tl} = -(5.11 \pm 1.06) \quad \text{J/(mol K)}.$$

According to the solid-phase diagram (Fig. 7), these functions are the thermodynamic characteristics of the following potential-forming reaction [15]:

$$Tl(solid) + 0.5TlBr(solid) + TlSe(solid) = 0.5Tl_5Se_2Br(solid).$$

Thus, the standard thermodynamic functions of formation and the standard entropy for the compound Tl_5Se_2Br can be calculated from

Table 3. Standard integral thermodynamic functions for compounds Tl_5Se_2Br, TlBr, and TlSe

Compound	$-\Delta G^0_{298}$	$-\Delta H^0_{298}$	ΔS^0_{298}	S^0_{298}
	kJ/mol		J/(mol K)	
TlBr [19]	167.40 ± ± 0.63	172.68 ± ± 0.67	–17.7 ± ± 1.2	122.59 ± ± 0.21
TlSe [20.21]	60.12 ± ± 0.10	60.96 ± ± 0.54	–2.8 ± ± 1.4	103.4 ± ± 1.8
Tl_5Se_2Br	374.3 ± 1.0	384.3 ± 2.7	–33.6 ± 6.0	447.6 ± 6.4

$$\Delta Z^0(Tl_5Se_2Br) = 2\Delta\bar{Z}_{Tl} + \Delta Z^0(TlBr) + 2\Delta Z^0(TlSe),$$

where $\Delta Z^0 - \Delta G^0$, ΔH^0, ΔS^0; and

$$S^0(Tl_5Se_2Br) = 2\Delta\bar{S}_{Tl} + 2S^0(Tl) + S^0(TlBr) + 2S^0(TlSe).$$

In so doing, we used our own $\Delta\bar{Z}_{Tl}$ data and borrowed from the literature the thermodynamic characteristics for TlBr [20] and TlSe [21] (Table 3) and the standard entropy of elementary thallium [20]. The results of the calculations are displayed in Table 3. The errors were found by error propagation.

REFERENCES

1. D. M. Babanly, Yu. A. Yusibov, and M. B. Babanly, Zh. Neorg. Khim. **52** (5) (2007) [Russ. J. Inorg. Chem. **52** (5), (2007)].
2. R. A. Alieva, I. M. Babanly, D. M. Babanly, and I. I. Aliev, Vestn. Bakinsk. Gos. Univ., Ser. Estestv. Nauki, No. 4, 35 (2004).
3. R. A. Alieva, I. M. Babanly, D. M. Babanly, and I. I. Aliev, Zh. Khim. Problem, No. 4, 83 (2004).
4. M. B. Babanly, G. M. Guseinov, D. M. Babanly, and F. M. Sadygov, Zh. Neorg. Khim. **57** (5), 876 (2006) [Russ. J. Inorg. Chem. **57** (5), 810 (2006)].
5. R. A. Alieva, I. M. Babanly, D. M. Babanly, and I. I. Aliev, Vestn. Bakinsk. Gos. Univ., Ser. Estestv. Nauki, No. 1, 42 (2005).
6. D. M. Babanly, A. A. Nadzhafova, M. I. Chiragov, and M. B. Babanly, Zh. Khim. Problem, No. 2, 149 (2005).
7. D. M. Babanly, G. M. Guseinov, Yu. A. Yusibov, and F. M. Sadygov, *Proceedings of the 9th Republican Conference "Physicochemical Analysis and Inorganic Materials Science,"* Baku, 2004 (Baku, 2004), p. 108 [in Russian].
8. D. M. Babanly, Z. G. Dzhafarova, and Yu. A. Yusibov, Vestn. Bakinsk. Gos. Univ., Ser. Estestv. Nauki, No. 1, 52 (2006).
9. R. Blachnik and Shch. A. Dreisbach, J. Alloys Compd. **52** (1), 53 (1984).

10. E. Yu. Peresh, V. B. Lazarev, and O. I. Korniichuk, et al., Neorg. Mater. **29** (3), 406 (1993).
11. Th. Doert and R. Asmuth, J. Alloys Compd. **209**, 151 (1994).
12. I. Schewe and P. Böttcher, Z. Kristallogr. **188** (2), 287 (1989).
13. *Handbuch der präparativen anorganischen Chemie*, Ed. by G. Brauer (Enke, Stuttgart, 1978; Mir, Moscow, 1985).
14. N. Kh. Abrikosov et al., *Semiconducting Chalcogenides and Their Base Alloys* (Nauka, Moscow, 1975) [in Russian].
15. M. B. Babanly, Yu. A. Yusibov, and V. T. Abishov, *Electromotive Forces in the Thermodynamics of Compound Semiconductors* (Baku State Univ., Baku, 1992) [in Russian].
16. L. I. Man, V. S. Parmon, R. M. Imanov, and A. S. Avilov, Kristallografiya **25** (5), 1070 (1980).
17. V. Ya. Anosov and S. A. Pogodin, *The Fundamentals of Physicochemical Analysis* (Nauka, Moscow/Leningrad, 1947) [in Russian].
18. K. Dreffel, *Statistics in Analytical Chemistry* (Mir, Moscow, 1994) [in Russian].
19. A. N. Kornilov, L. B. Stepina, and V. A. Sokolov, Zh. Fiz. Khim. **46** (11), 2974 (1972).
20. *Thermal Constants of Compounds. Handbook*, Ed. by V. P. Glushko (VINITI, Moscow, 1971), Vol. V [in Russian].
21. V. P. Vasil'ev, A. V. Nikol'skaya, and Ya. I. Gerasimov, Zh. Fiz. Khim. **45** (8), 2061 (1971).